

Cooperative demethylation by JMJD2C and LSD1 promotes androgen receptor-dependent gene expression

Melanie Wissmann¹, Na Yin¹, Judith M. Müller¹, Holger Greschik¹, Barna D. Fodor², Thomas Jenuwein², Christine Vogler³, Robert Schneider³, Thomas Günther¹, Reinhard Buettner⁴, Eric Metzger¹ and Roland Schüle^{1,5}

Posttranslational modifications of histones, such as methylation, regulate chromatin structure and gene expression¹. Recently, lysine-specific demethylase 1 (LSD1)², the first histone demethylase, was identified. LSD1 interacts with the androgen receptor and promotes androgen-dependent transcription of target genes by ligand-induced demethylation of mono- and dimethylated histone H3 at Lys 9 (H3K9)³ only. Here, we identify the Jumonji C (JMJC)⁴ domain-containing protein JMJD2C^{5,6} as the first histone tridemethylase regulating androgen receptor function. JMJD2C interacts with androgen receptor *in vitro* and *in vivo*. Assembly of ligand-bound androgen receptor and JMJD2C on androgen receptor-target genes results in demethylation of trimethyl H3K9 and in stimulation of androgen receptor-dependent transcription. Conversely, knockdown of JMJD2C inhibits androgen-induced removal of trimethyl H3K9, transcriptional activation and tumour cell proliferation. Importantly, JMJD2C colocalizes with androgen receptor and LSD1 in normal prostate and in prostate carcinomas. JMJD2C and LSD1 interact and both demethylases cooperatively stimulate androgen receptor-dependent gene transcription. In addition, androgen receptor, JMJD2C and LSD1 assemble on chromatin to remove methyl groups from mono, di and trimethylated H3K9. Thus, our data suggest that specific gene regulation requires the assembly and coordinate action of demethylases with distinct substrate specificities.

The amino-terminal tails of histones are subject to a plethora of post-translational modifications (such as acetylation, phosphorylation, ubiquitination and methylation) by specific chromatin-modifying enzymes¹. Lysine residues in histone tails can be mono, di or trimethylated. The differentially methylated lysine residues serve as docking sites for various effector proteins and chromatin modifiers, which results in diverse physiological responses, such as transcriptional repression and activation^{1,7-9}. The recent identification of lysine-specific histone demethylases, such as the amine oxidase LSD1 (refs 2, 3) and the JMJC

domain-containing hydroxylases demonstrates that histone methylation is reversible and dynamically regulated^{4-6,10-14}. We have previously shown that LSD1 interacts with the androgen receptor and promotes ligand-dependent transcription of androgen receptor target genes resulting in enhanced tumour-cell growth. Ligand-induced activation of androgen receptor target genes demands the removal of the repressive histone marks, mono, di and trimethyl histone H3 at Lys 9 (H3K9). However, LSD1 removes only mono and dimethyl but not trimethyl groups from H3K9 (ref. 3). Thus, ligand-induced demethylation of trimethyl H3K9 and subsequent androgen receptor target gene activation requires an as yet unidentified specific histone tridemethylase.

Using a candidate approach¹¹ to discover such a tridemethylase, we identified JMJD2C^{5,6}. To investigate whether JMJD2C colocalizes with androgen receptor, we used immunohistochemical analyses of prostate and prostate tumour biopsies on tissue microarrays. JMJD2C was detected in the epithelium of normal prostate and in prostate carcinoma cells (Fig. 1A). These cells also express LSD1, demonstrating that JMJD2C not only colocalizes with androgen receptor, but also with the demethylase LSD1 (Fig. 1A and see Supplementary Information, Fig. S1a). Furthermore, as shown in coimmunoprecipitation assays, endogenous JMJD2C and androgen receptor specifically associate in the prostate (Fig. 1B). Importantly, JMJD2C also interacts with LSD1 *in vivo* (Fig. 1B and see Supplementary Fig. S1b). To demonstrate that all three proteins exist in a single protein complex, a TAP-based copurification strategy was used (Fig. 1C). 293 cells were transfected with Flag-tagged androgen receptor (Flag-AR), V5-JMJD2C, and either TAP-LSD1 or TAP (Fig. 1C, a). The TAP-LSD1-associated protein complexes were immobilized on IgG-Sepharose and the presence of both androgen receptor and JMJD2C in the immobilized LSD1 complexes was verified by western-blot analysis (Fig. 1C, b). Androgen receptor and JMJD2C did not copurify in the presence of the TAP control, demonstrating specific association of androgen receptor and JMJD2C with TAP-LSD1 (Fig. 1C, b). LSD1-associated complexes were released from IgG-Sepharose by TEV protease cleavage of the TAP-tag (Fig. 1C, c) followed by immunoprecipitation of Flag-tagged androgen receptor with

¹Universitäts-Frauenklinik und Zentrum für Klinische Forschung, Klinikum der Universität Freiburg, Breisacherstrasse 66, 79106 Freiburg, Germany.

²Research Institute of Molecular Pathology (IMP), The Vienna Biocenter, Dr. Bohrgasse 7, 1030 Vienna, Austria. ³Max-Planck-Institut für Immunbiologie, Stübweg 51, 79108 Freiburg, Germany. ⁴Institut für Pathologie, Universitätsklinikum Bonn, Sigmund-Freud-Strasse 25, 53127 Bonn, Germany.

⁵Correspondence should be addressed to R.S. (e-mail: roland.schuele@uniklinik-freiburg.de)

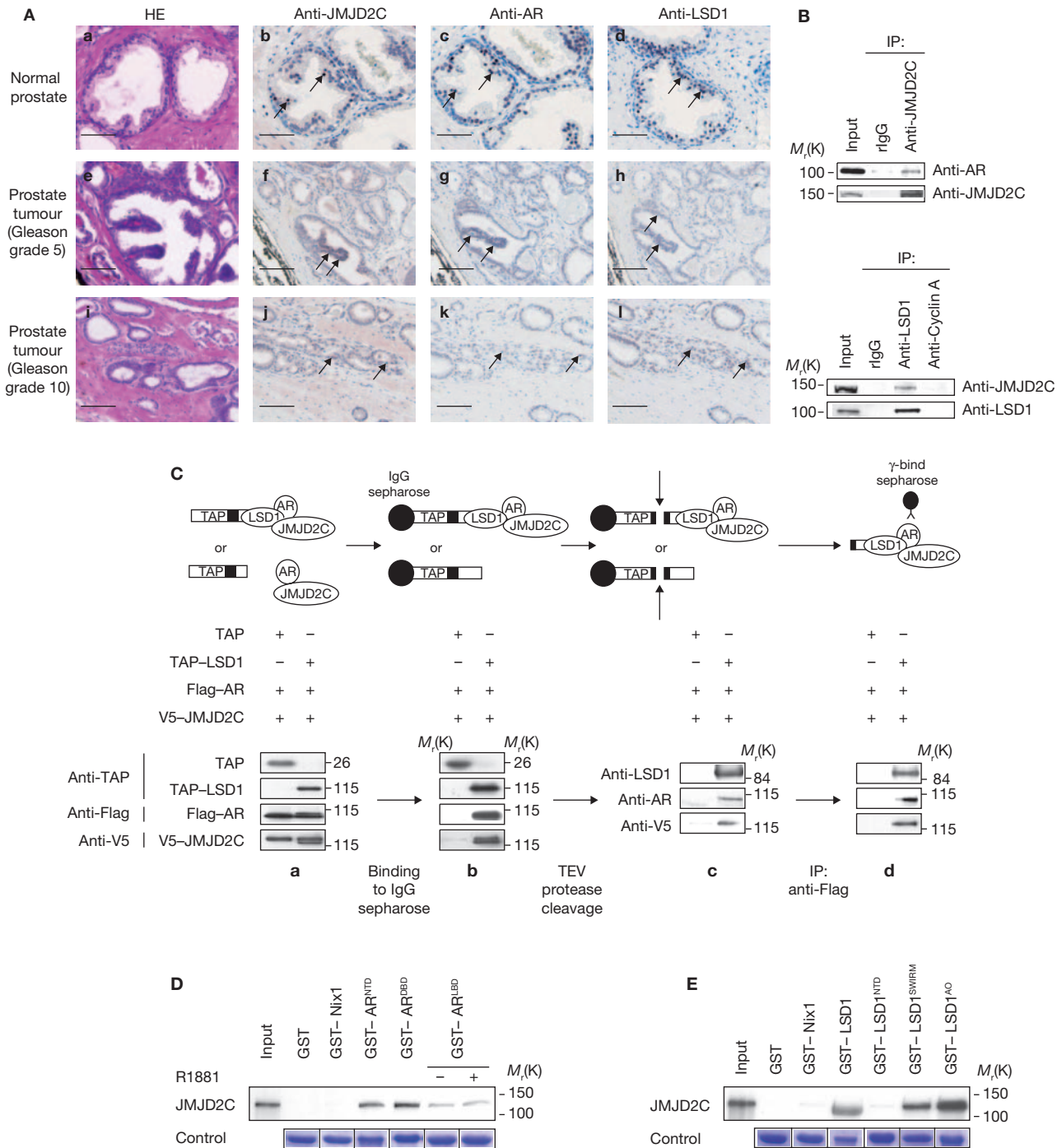


Figure 1 JMJD2C colocalizes and interacts with both androgen receptor and LSD1. **(A)** Immunohistochemical staining of JMJD2C, androgen receptor and LSD1 in normal human prostate and tumour human prostate. JMJD2C (b, f, j), androgen receptor (c, g, k), and LSD1 (d, h, l) immunoreactivity is detected in the secretory epithelium of normal prostate (b–d; arrows) and prostate carcinoma cells (f–l; arrows). Hematoxylin-eosin (HE) stained sections are shown in a, e and i. All sections were taken from the same radical prostatectomy specimen. Magnification: $\times 250$. **(B)** JMJD2C interacts with androgen receptor and LSD1 *in vivo*. Extracts from mouse prostate were immunoprecipitated with either anti-JMJD2C, anti-LSD1, anti-cyclin A antibodies or rabbit IgG. Western blots were probed with anti-androgen receptor, anti-JMJD2C or anti-LSD1 antibodies as indicated. **(C)** JMJD2C, LSD1 and androgen receptor are present in a single protein complex. A schematic representation of the experimental strategy is shown in the upper part of the figure. 293 cells were transfected with expression plasmids for

V5-JMJD2C, Flag-AR, and either TAP-LSD1 or TAP, as indicated. Protein complexes were immobilised on IgG-Sepharese, released from IgG-Sepharese by TEV protease cleavage of the TAP tag, followed by immunoprecipitation of Flag-tagged androgen receptor with anti-Flag antibody. The presence of LSD1 and JMJD2C in association with androgen receptor was confirmed by western blotting with anti-LSD1, anti-androgen receptor and anti-V5 antibodies, respectively. Ten percent of the extract used for immunoprecipitation was loaded as input. **(D, E)** GST pull-down assays were performed with labelled JMJD2C and the bacterially expressed and purified GST-AR fusion proteins, GST-LSD1 or fusion proteins thereof. GST and GST-Nix1 proteins were used as control. AO, amine oxidase domain. Coomassie blue staining shows the amounts of GST-fusion proteins used. The individual Coomassie bands representing the different GST fusion proteins are shown and uncropped images of the scans are shown in the Supplementary Information, Fig. S7. The scale bars represent 100 μm in **A**, a–e and 200 μm in **A**, f–l.

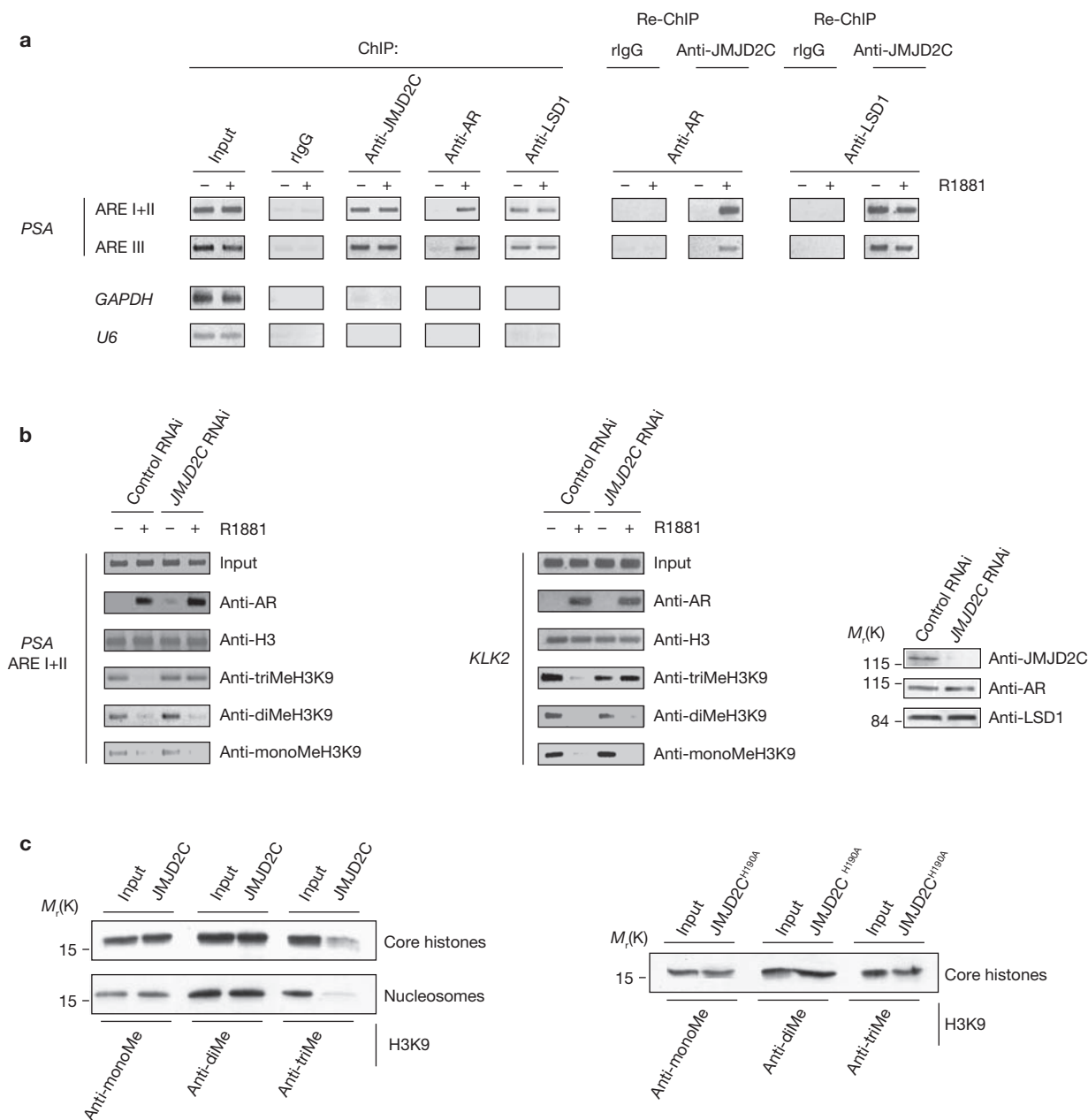


Figure 2 JMJD2C interacts with chromatin and demethylates H3K9. (a, b) LNCaP cells were incubated with or without the androgen-receptor agonist R1881 (a, b) and transfected with stealth RNAi (b). ChIP or re-ChIP was performed with the indicated antibodies. The precipitated chromatin was amplified by PCR using primers flanking the promoter region (ARE I+II) and the enhancer region (ARE III) of the *PSA* gene, the promoter region (ARE) of the *KLK2* gene, or the promoters of the unrelated *GAPDH* and *U6*

genes. Western blot analysis (b, right panel) verified the specific siRNA-mediated knockdown of *JMJD2C*. (c) Core histones or nucleosomes from HeLa cells were incubated with recombinant JMJD2C (amino acids 12–349) or mutant JMJD2C^{H190A} (amino acids 12–349). Western blots were probed with the indicated antibodies against anti-mono, anti-di, or anti-trimethyl H3K9. Uncropped images of the scans are shown in the Supplementary Information, Fig. S7.

anit-Flag antibody. The specific association of JMJD2C and LSD1 with androgen receptor in a single protein complex was verified by western-blot analysis (Fig. 1C, d). The TAP-based copurification strategy was used because the moderate expression levels of the endogenous proteins would only have allowed a limited number of purification steps. Therefore, using common methodology (such as gel filtration and density gradient centrifugation) would have left the possibility that two very similar, yet distinct complexes (for example, one containing androgen receptor and JMJD2C, the other containing androgen receptor and LSD1), could have been copurified.

GST pulldown analyses showed that full-length JMJD2C directly interacts with the amino-terminal domain (NTD), the DNA-binding domain (DBD) and the ligand-binding domain (LBD) of androgen receptor (Fig. 1D and see Supplementary Information, Fig. S2a, b). JMJD2C did not associate with the control GST or GST-Nix1, thus demonstrating specificity of interaction with androgen receptor *in vitro*. In addition, JMJD2C interacted with full-length LSD1. The association with JMJD2C is mediated by the centrally located SWIRM domain, and the carboxy-terminal amine oxidase domain, which harbours the demethylase activity² (Fig. 1E and see Supplementary Information,

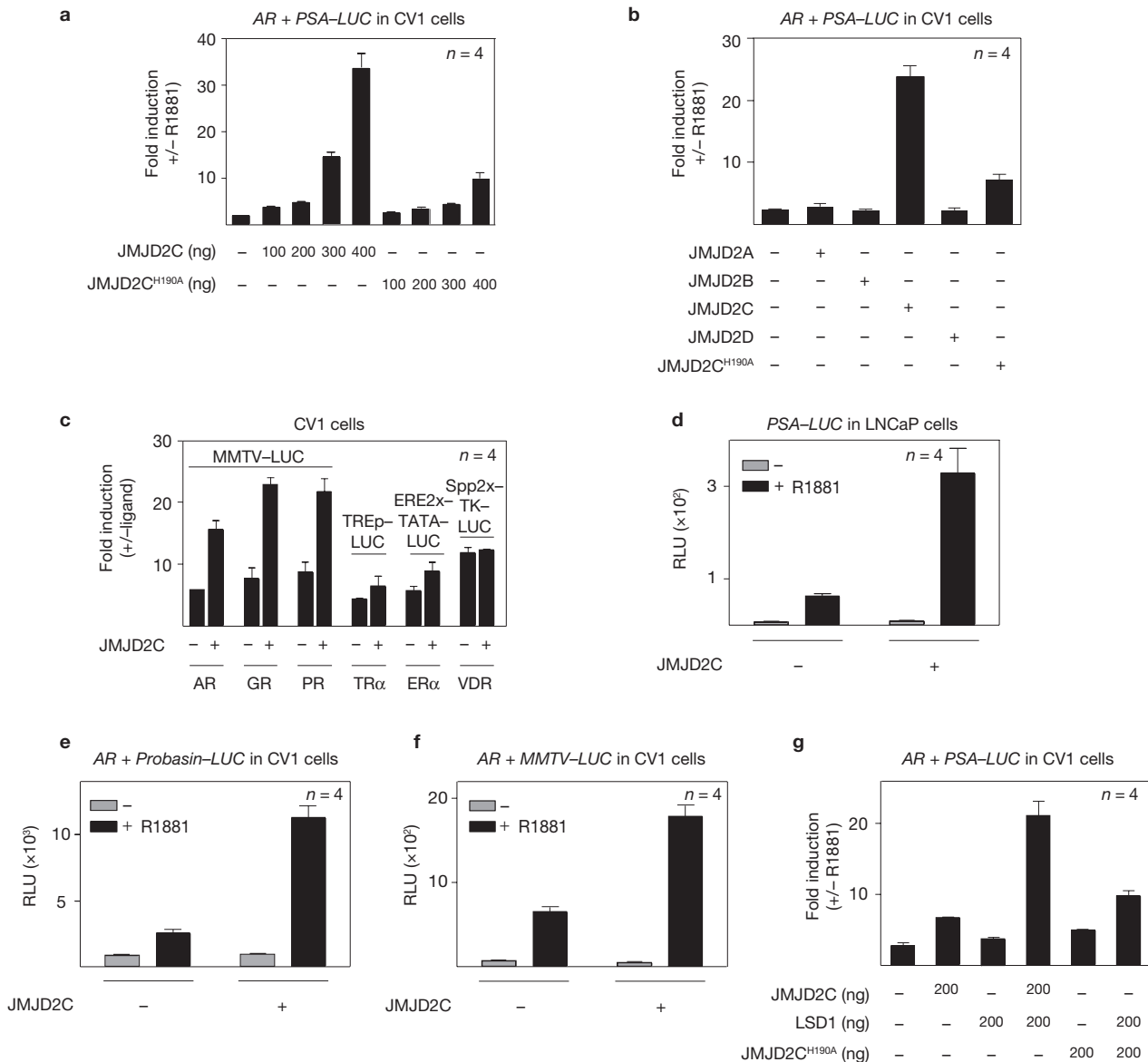


Figure 3 JMJD2C controls androgen receptor-induced transcriptional activity. (**a–g**) CV1 (**a–c, e–g**) or LNCaP (**d**) cells were transfected with androgen receptor-dependent reporters in the presence or absence of R1881. CV1 cells were cotransfected with androgen-receptor expression plasmid (**a, b, c, e, f, g**). In **c**, CV1 cells were transfected with the indicated receptors and reporters and incubated in the presence or absence of either R1881, Dex, R5020, T3, E2 or Vit D. JMJD2C, but not the other

JMJD2 family members JMJD2A, JMJD2B or JMJD2D (**b**), controls androgen receptor-induced transcriptional activity on different natural androgen receptor-regulated promoters and cell lines (**a, b, d–f**). JMJD2C also regulates the transcriptional activity of other nuclear receptor family members (**c**). Limited amounts (200 ng) of JMJD2C, JMJD2C^{H190A} or LSD1 were tested for co-operative stimulation of androgen receptor-dependent reporter activity (**g**). The error bars represent mean + s.d. ($n \geq 5$).

Fig. S2c). Taken together, our data show that JMJD2C, androgen receptor and LSD1 are not only coexpressed in the prostate, but also interact *in vitro* and *in vivo*.

To determine whether JMJD2C associates with chromatin *in vivo*, LNCaP human prostate tumour cells were subjected to chromatin immunoprecipitation (ChIP) in the presence or absence of the androgen receptor agonist, R1881. JMJD2C associated with the androgen response elements (ARE I+II and ARE III) located in the promoter and enhancer of the prostate specific antigen (PSA) gene in a ligand-independent manner (Fig. 2a and see Supplementary Information, Fig. S3a). This association is specific, as the promoters of the unrelated *GAPDH* and *U6* genes were not enriched. Androgen receptor occupied the AREs of the PSA

gene only in the presence of ligand (Fig. 2a and see ref. 3). To demonstrate that JMJD2C and androgen receptor form a complex on the PSA promoter, R1881-treated LNCaP cells were subjected to sequential ChIP (Re-ChIP), first with anti-androgen receptor antibody and then with anti-JMJD2C antibody. Importantly, both ARE-containing regions were specifically enriched, demonstrating that JMJD2C and ligand-bound androgen receptor formed a complex on chromatin (Fig. 2a). As shown previously, LSD1 associated with chromatin both in the presence and absence of ligand (Fig. 2a and ref. 3). Notably, Re-ChIP experiments demonstrated that JMJD2C and LSD1 assembled together on the AREs of the PSA promoter (Fig. 2a). In summary, these data suggest the assembly of ligand-bound androgen receptor, JMJD2C and LSD1 into a multiple-specificity demethylase complex.

As androgen-stimulated transcription is accompanied by a robust decrease in mono, di and trimethyl H3K9 at the *PSA* promoter³, we examined whether JMJD2C executes the ligand-dependent demethylation of trimethyl H3K9. Transfection of LNCaP cells with small interference RNAs (siRNAs) directed against *JMJD2C* efficiently blocked ligand-dependent demethylation of trimethyl H3K9 at the *PSA* promoter, but not that of mono and dimethyl H3K9 (Fig. 2b). JMJD2C knockdown was specific and did not affect the level of endogenous androgen receptor and LSD1, or the protein levels of the other JMJD2 family members (Fig. 2b and see Supplementary Information, Fig. S3b). Furthermore, the amount of total H3 on the *PSA* promoter was not influenced by JMJD2C knockdown and the methylation status of H3K9 was not altered by an unrelated control siRNA (Fig. 2b). Similar results were obtained with the androgen receptor-regulated *Kallikrein* (*KLK2*) promoter¹⁵ (Fig. 2b). To further confirm that JMJD2C specifically removes trimethyl H3K9 marks, demethylation assays were performed *in vitro*. Recombinantly expressed and purified JMJD2C was incubated with either core histones or HeLa nucleosomes as substrates (Fig. 2c and see Supplementary Information, Fig. S3c). Recombinant JMJD2C very efficiently demethylated trimethyl H3K9 on both core histones and nucleosomes *in vitro*, whereas the methylation status of mono and dimethyl H3K9 was not altered, corroborating demethylation results obtained with trimethyl H3K9 peptide as a substrate^{5,6}. As expected, the enzymatically impaired mutant JMJD2C^{H190A} (ref. 5) failed to demethylate (Fig. 2c and see Supplementary Information, Fig. S3c). Taken together, these data show the specific demethylation of the repressive histone mark, trimethyl H3K9, by JMJD2C.

Next, transient transfection assays were performed to determine whether JMJD2C modulates the transcriptional activity of androgen receptor. Coexpression of androgen receptor and increasing amounts of JMJD2C resulted in a strong ligand-dependent activation of a *PSA* luciferase reporter (Fig. 3a), which was not observed in the absence of either ligand (Fig. 3a) or of androgen receptor (see Supplementary Information, Fig. S4a). In addition, other members of the JMJD2 family did not influence the transcriptional activity of androgen receptor (Fig. 3b). Interestingly, JMJD2C also activates other members of the nuclear receptor superfamily, such as glucocorticoid receptor and progesterone receptor, but not thyroid receptor α (TR α), oestrogen receptor α (ER α), or vitamin D receptor (VDR; Fig. 3c). Stimulation of androgen-receptor activity by JMJD2C is potent in different cell lines, and various androgen receptor-responsive promoters are activated by JMJD2C in a ligand-dependent manner (Fig. 3d–f). The fact that JMJD2C and LSD1 are coexpressed in prostate cells and assemble in a complex on the *PSA* promoter *in vivo* suggested a functional cooperativity between these two demethylases. To address this issue, we tested limited amounts of LSD1 or JMJD2C, which alone only weakly stimulated ligand-dependent androgen receptor activity (Fig. 3g). Coexpression of limited amounts of both demethylases induced robust co-operative stimulation of androgen receptor transcriptional activity (Fig. 3g). In contrast, coexpression of LSD1 and the mutant JMJD2C^{H190A} resulted in a weak superactivation of androgen receptor (Fig. 3g). Taken together, these data show that demethylases with different substrate specificities co-operate to stimulate androgen receptor-dependent gene expression.

As removal of the repressive histone mark, trimethyl H3K9, by JMJD2C increases androgen receptor-dependent gene expression, knockdown of JMJD2C should reduce the expression of endogenous

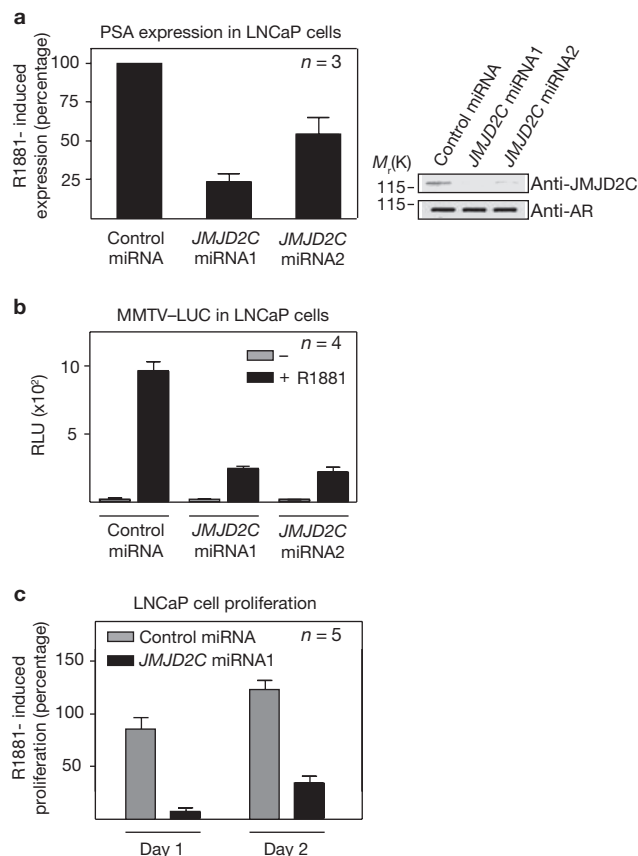


Figure 4 JMJD2C knockdown blocks androgen receptor-induced transcriptional activity and tumour cell proliferation. (a–c) In LNCaP cells, miRNA-mediated JMJD2C knockdown reduces expression of the endogenous *PSA* gene (a, left panel), androgen receptor-dependent reporter activity (b) and R1881-induced cell proliferation (c). Knockdown of JMJD2C was verified by western blot analysis (a, right panel) using anti-JMJD2C or anti-androgen receptor antibodies. The error bars represent mean + s.d. ($n \geq 4$). Uncropped images of the scans are shown in the Supplementary Information, Fig. S7.

androgen-receptor target genes. To test this hypothesis, LNCaP cells were infected with lentiviruses expressing micro RNA (miRNA) directed against *JMJD2C*. This resulted in efficient and specific downregulation of endogenous JMJD2C (Fig. 4a). Quantitative RT-PCR analyses demonstrated that knockdown of JMJD2C blocks androgen-induced expression of endogenous androgen-receptor target genes, such as *PSA* or *KLK2*, in LNCaP cells (Fig. 4a and see Supplementary Information, Fig. S4b). Similarly, vector-mediated JMJD2C knockdown by the same miRNAs resulted in a strong ligand-dependent decrease of *MMTV-LUC* reporter gene expression (Fig. 4b). To address whether JMJD2C governs androgen-dependent cell growth, proliferation of pLenti6-JMJD2C miRNA-infected LNCaP cells was analysed. When compared with cells infected with the virus expressing an unrelated control miRNA, androgen-induced proliferation of LNCaP cells was dramatically reduced by JMJD2C knockdown (Fig. 4c). These results demonstrate the importance of JMJD2C in the control of androgen-induced gene regulation and cell proliferation.

Taken together, our data show that the trimethyl-specific histone demethylase JMJD2C controls androgen-receptor function. JMJD2C and ligand-bound androgen receptor associate at androgen-regulated promoters, which results in specific demethylation of the repressive

histone mark trimethyl H3K9. Importantly, we have unravelled a novel mechanism by which the co-operative action of the two demethylases, JMJD2C and LSD1, leads to removal of the repressive mono, di and trimethyl marks on H3K9. Thus, the action of a multiple demethylation complex with distinct substrate specificities allows the optimal activation of androgen-receptor target genes. Notably, both JMJD2C and LSD1 are coexpressed with androgen receptor in human prostate tumours, and reduction of either LSD1 (ref. 3) or JMJD2C severely inhibits androgen-dependent proliferation of prostate tumour cells. Thus, specific modulation of JMJD2C activity alone, or in combination with LSD1, may be a promising therapeutic strategy to control androgen-receptor activity in tissues where androgen receptor has a pivotal physiological role. □

METHODS

Plasmids. The following plasmids were described previously: pSG5-AR, CMX-Flag, GST-AR-NTD, GST-AR-DBD, GST-AR-LBD, progesterone receptor, glucocorticoid receptor, VDR, MMTV-LUC, Spp2x-TK-LUC, Probasin-LUC and PSA-LUC¹⁶; GST-LSD1, GST-LSD1-NTD, GST-LSD1-SWIRM, GST-LSD1-AO, GST-Nix1, ER α , TREp-LUC and ERE2x-TATA-LUC, TAP, TAP-LSD1 and Flag-AR³; and pJAL-JMJD2A¹⁷. To construct CMX-Flag-JMJD2C, CMX-Flag-JMJD2C^{H190A}, CMX-Flag-JMJD2D, CMX-DEST51-JMJD2B, CMX-DEST51-JMJD2C, pRSET-JMJD2C (amino acids 12–349) and pRSET-JMJD2C^{H190A} (amino acids 12–349), the corresponding fragments were inserted into pCMX-Flag, pCMX-DEST51, pGEX4T-1 or pRSET. To construct pLenti6-JMJD2C miRNA, pLenti6-JMJD2C miRNA2, pGW-JMJD2C miRNA and pGW-JMJD2C miRNA, the DNA corresponding to JMJD2C miRNA (5'-TGCTGAAATGCATCACACCC TTGGGAGT TTTGGCCACTGACTGACTCCCAAGGGTGATGCATTT-3' and 5'-CCTGAAATGCATCACCCCTGGGAGTCACTGAGTGCACAAAACCTCCC AAGGGTGTGATGCATTT-3') and JMJD2C miRNA2 (5'-TGCTGTAAAGCAG CTGTTTCTCTGAGAGT TTTGGCCACTGACTGACTCTCAGGACAGCTGCT TAA-3' and 5'-CCTGTAAAGCAGCTGCTGCTGAGATCAGTCACTGGCC CAAAACCTCTCAGGAAACAGCTGCTTAAC-3') was cloned into pLenti6-V5-DEST and pcDNA-6.2-GW-EmGFP according to the manufacturer's instruction (Invitrogen, Karlsruhe, Germany). Cloning details can be obtained on request.

Cell culture and transfection. CV1 and LNCaP cells were cultured and transfected as previously described¹⁸. The following amounts were transfected per well: 500 ng MMTV-LUC, PSA-LUC, Probasin-LUC, TREp-LUC, ERE2x-TATA-LUC, or Spp2x-TK-LUC; 25 ng androgen receptor, progesterone receptor, glucocorticoid receptor, TR α , ER α or VDR expression plasmid; 200 ng (Fig. 3g) or 400 ng (Fig. 3b–f) expression plasmids of LSD1, JMJD2A/B/C/D or JMJD2C^{H190A}, 1 μ g expression plasmid of control miRNA, JMJD2C miRNA1 or JMJD2C miRNA2. Cells were treated in the presence or absence of 10⁻¹⁰ M R1881, 10⁻⁷ M R5020, 10⁻⁷ M dexamethasone (Dex), 10⁻⁷ M estradiol (E2), 10⁻⁷ M thyroid hormone (T3), 10⁻⁷ M vitamin D (Vit D; Sigma, Taufkirchen, Germany) for 18 h, as indicated. Luciferase activity was assayed as previously described¹⁸. All experiments were repeated at least five times in duplicate.

Immunohistochemistry. Polyclonal rabbit anti-JMJD2C antibody was generated according to standard procedures. Stainings were performed using a protocol¹⁹ for antigen retrieval and indirect immunoperoxidase. Anti-androgen receptor 441 (Santa Cruz, Heidelberg, Germany), anti-LSD1 (ref. 3), and anti-JMJD2C antibodies were used at dilutions of 1:75, 1:500 and 1:50, respectively. Rabbit and mouse IgG were used as secondary antibodies (1:500; Dako, Glostrup, Denmark). Immunoreactions were visualised with the ABC complex diluted 1:50 in PBS (Vectastain; Vector, Burlingame, CA).

Chromatin immunoprecipitation. ChIP experiments were performed as previously described³. LNCaP cells were treated for 45 min (Fig. 2a) or 210 min in the presence or absence of 10⁻⁸ M R1881, as indicated. LNCaP cells were transfected three days before harvesting for ChIP, with or without stealth RNAi (Invitrogen), following the manufacturer's instructions. Immunoprecipitation was performed with specific antibodies (anti-monoMeH3K9, anti-diMeH3K9, anti-triMeH3K9, anti-H3, anti-androgen receptor PG21 (Upstate Biotechnology, Charlottesville,

VA), anti-LSD1 (ref. 3) and anti-JMJD2C) on GammaBind-Sepharose 4B (GE-Healthcare, Munich, Germany). For PCR, 1–5 μ l out of 50 μ l DNA extract was used. For re-ChIP assays, immunoprecipitations were sequentially washed with TSE I, TSE II, buffer III and TE (ref. 20). Complexes were eluted by incubation with 10 mM DTT at 37 °C for 30 min, diluted 50 times with dilution buffer²⁰, followed by a second immunoprecipitation with the indicated antibodies. PCR primers for ARE I+II (PSA -459 to -121), ARE III (PSA -4288 to -3922), GAPDH and U6 were described previously³. Primer sequences for the promoter region (-343 to -90) of the KLK2 gene are as follows: 5'-ACCCCTGTGCTGTTTCATCCTG-3' and 5'-CCGCCCTTGCCCTGTTGG-3'.

Coimmunoprecipitation assay and western blot analysis. Experiments were performed as previously described¹⁶. Immunoprecipitations from extracts of mouse prostate were performed in the presence of 10⁻¹⁰ M R1881 with either anti-JMJD2C, anti-LSD1 (ref. 3), anti-cyclin A¹⁹ antibodies or rabbit IgG. Western blots were probed as indicated including anti-androgen receptor antibody (N-20, Santa Cruz). Of the prostate extract used for the coimmunoprecipitation, 1.5% was loaded as input.

In vitro pulldown assay. GST pulldown assays were performed with equal amounts of GST or GST-fusion proteins as previously described¹⁹ using buffer containing 150 mM KCl and 0.15% NP-40. Ten percent of the *in vitro*-translated proteins used for the pulldown were loaded as input.

Cell-proliferation assay. Experiments were performed as previously described³. pLenti6-control miRNA and pLenti6-JMJD2C miRNA1 were used to produce recombinant lentiviruses to infect LNCaP cells as previously described²¹. The infected cells were cultured for 72 h in medium containing 10% double-stripped FCS. Cells (1 \times 10⁴) were plated in 96-well plates in the presence or absence of 10⁻⁹ M R1881. The cell proliferation ELISA BrdU colorimetric assay (Roche, Mannheim, Germany) was performed according to the manufacturer's instructions. The percentage increase in proliferation in the presence versus absence of R1881 is shown. The experiment was performed in quintuplicate.

Quantitative RT-PCR and statistical analysis. Quantitative RT-PCR and statistical analysis were performed as previously described³. The primers for GAPDH and PSA were described previously³.

In vitro demethylation assay. The demethylation assays were performed as previously described⁴. His-tagged proteins were incubated for 5 h at 37 °C in demethylation buffer containing 50 mM HEPES-KOH at pH 8.0, 2 mM ascorbate, 100 μ M Fe(NH₄)₂(SO₄)₂, 1 mM α -ketoglutarate with 1 μ g of core histones (Sigma) or nucleosomes purified from HeLa cells²². The reaction mixture was analysed by SDS-PAGE followed by western blotting using antibodies as indicated.

Tandem affinity purification. TAP purification was essentially performed as previously described²³. Nuclear extracts from 293 cells transfected with Flag-AR, V5-JMJD2C, and either TAP-tag-LSD1 (TAP-LSD1) or control TAP-tag (TAP) were prepared in SC buffer (50 mM Tris-HCl at pH 8, 170 mM NaCl, 20% glycerol, 0.2 mM DTT, 0.1% NP-40, 10⁻⁹ M R1881, 50 mM NaF, 2 mM Na₃VO₄, and complete protease inhibitor cocktail). TAP-tagged proteins were bound to IgG-Sepharose (GE-Healthcare) in SC buffer at 4 °C overnight, followed by repeated washing. Bound complexes were released from IgG-Sepharose by TEV-protease cleavage (100 U, Invitrogen) in TEV buffer (10 mM Tris-HCl at pH 8.0, 150 mM NaCl, 0.1% NP40, 1 mM DTT, 1 mM EDTA, 10⁻⁹ M R1881). Immunoprecipitation was performed with anti-Flag antibody.

Note: Supplementary Information is available on the Nature Cell Biology website.

ACKNOWLEDGEMENTS

We thank S. Gray for generously providing reagents. We thank K. Fischer, L. Walz, F. Klott and S. Vomstein for excellent technical assistance. We are obliged to M. Hoffmann and A. Schwentek from the sequencing core facility. We thank M. Follo for help with editing the manuscript. This work was supported by grants from the Deutsche Forschungsgemeinschaft (SFB 747/P2, Schu 688/7-1, and Schu 688/9-1), the Dr. Hans Messner-Stiftung, and the Deutsche Krebshilfe (10-2019-Bu 1) to R.S.

COMPETING FINANCIAL INTERESTS

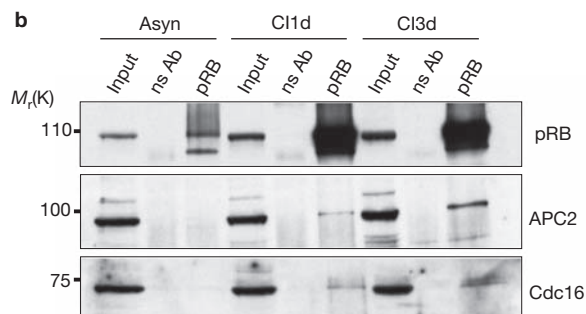
The authors declare that they have no competing financial interests.

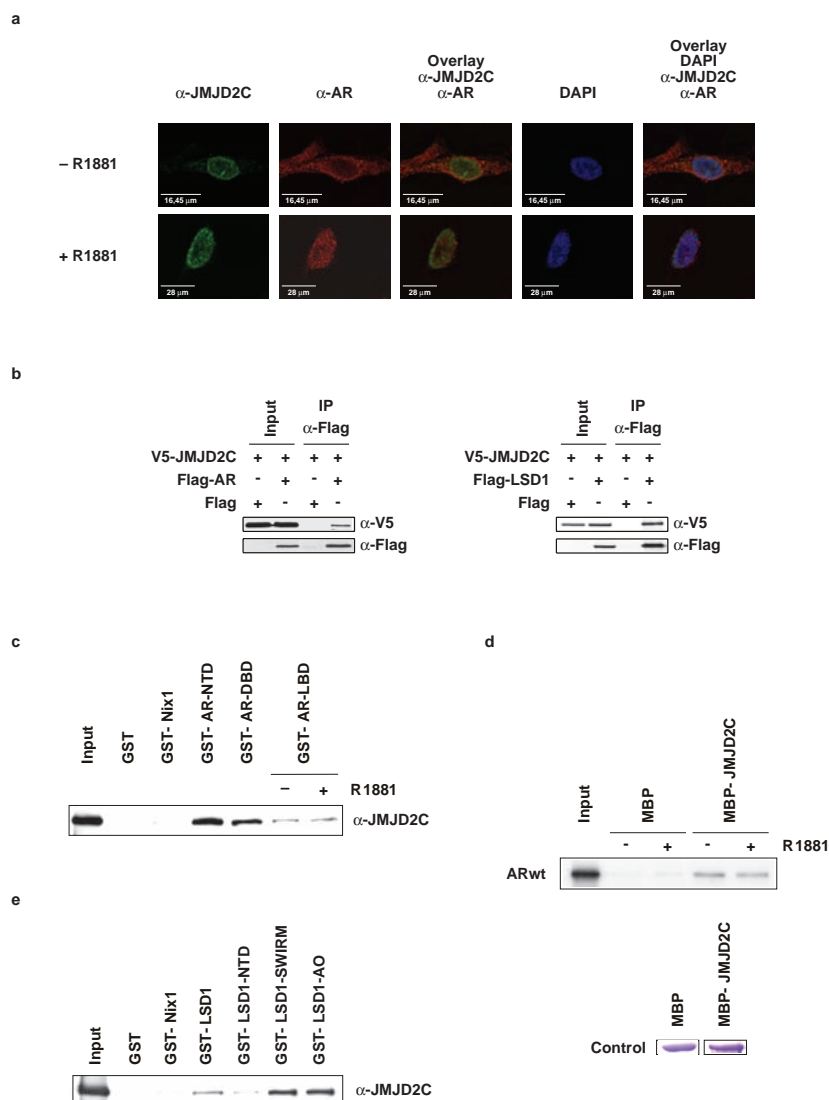
Published online at <http://www.nature.com/naturecellbiology/>
 Reprints and permissions information is available online at <http://npg.nature.com/reprintsandpermissions/>

1. Strahl, B. D. & Allis, C. D. The language of covalent histone modifications. *Nature* **403**, 41–45 (2000).
2. Shi, Y. *et al.* Histone demethylation mediated by the nuclear amine oxidase homolog LSD1. *Cell* **119**, 941–953 (2004).
3. Metzger, E. *et al.* LSD1 demethylates repressive histone marks to promote androgen-receptor-dependent transcription. *Nature* **437**, 436–439 (2005).
4. Tsukada, Y. I. *et al.* Histone demethylation by a family of JmjC domain-containing proteins. *Nature* **435**, 811–816 (2005).
5. Whetstine, J. R. *et al.* Reversal of histone lysine trimethylation by the JMJD2 family of histone demethylases. *Cell* **125**, 467–481 (2006).
6. Cloos, P. A. *et al.* The putative oncogene GASC1 demethylates tri- and dimethylated lysine 9 on histone H3. *Nature* **442**, 307–311 (2006).
7. Shi, X. *et al.* ING2 PHD domain links histone H3 lysine 4 methylation to active gene repression. *Nature* **442**, 96–99 (2006).
8. Wysocka, J. *et al.* A PHD finger of NURF couples histone H3 lysine 4 trimethylation with chromatin remodelling. *Nature* **442**, 86–90 (2006).
9. Rosenfeld, M. G., Lunyak, V. V. & Glass, C. K. Sensors and signals: a coactivator/corepressor/epigenetic code for integrating signal-dependent programs of transcriptional response. *Genes Dev.* **20**, 1405–1428 (2006).
10. Yamane, K. *et al.* JHDM2A, a JmjC-containing H3K9 demethylase facilitates transcription activation by androgen receptor. *Cell* **125**, 483–495 (2006).
11. Trewick, S. C., McLaughlin, P. J. & Allshire, R. C. Methylation: lost in hydroxylation? *EMBO Rep.* **6**, 315–320 (2005).
12. Fodor, B. D. *et al.* Jmjd2b antagonizes H3K9 trimethylation at pericentric heterochromatin in mammalian cells. *Genes Dev.* **20**, 1557–1562 (2006).
13. Klose, R. J. *et al.* The transcriptional repressor JHDM3A demethylates trimethyl histone H3 lysine 9 and lysine 36. *Nature* **442**, 312–316 (2006).
14. Trojer, P. & Reinberg, D. Histone lysine demethylases and their impact on epigenetics. *Cell* **125**, 213–217 (2006).
15. Kang, Z., Pirskanen, A., Janne, O. A. & Palvimo, J. J. Involvement of proteasome in the dynamic assembly of the androgen receptor transcription complex. *J. Biol. Chem.* **277**, 48366–48371 (2002).
16. Metzger, E., Müller, J. M., Ferrari, S., Buettner, R. & Schüle, R. A novel inducible transactivation domain in the androgen receptor: implications for PRK in prostate cancer. *EMBO J.* **22**, 270–280 (2003).
17. Gray, S. G. *et al.* Functional characterization of JMJD2A, a histone deacetylase- and retinoblastoma-binding protein. *J. Biol. Chem.* **280**, 28507–28518 (2005).
18. Müller, J. M. *et al.* The transcriptional coactivator FHL2 transmits Rho signals from the cell membrane into the nucleus. *EMBO J.* **21**, 736–748 (2002).
19. Müller, J. M. *et al.* FHL2, a novel tissue-specific coactivator of the androgen receptor. *EMBO J.* **19**, 359–369 (2000).
20. Shang, Y., Myers, M. & Brown, M. Formation of the androgen receptor transcription complex. *Mol. Cell* **9**, 601–610 (2002).
21. Wiznerowicz, M. & Trono, D. Conditional suppression of cellular genes: lentivirus vector-mediated drug-inducible RNA interference. *J. Virol.* **77**, 8957–8961 (2003).
22. O'Neill, T. E., Roberge, M. & Bradbury, E. M. Nucleosome arrays inhibit both initiation and elongation of transcripts by bacteriophage T7 RNA polymerase. *J. Mol. Biol.* **223**, 67–78 (1992).
23. Rigaut, G. *et al.* A generic protein purification method for protein complex characterization and proteome exploration. *Nature Biotechnol.* **17**, 1030–1032 (1999).

CORRIGENDUM

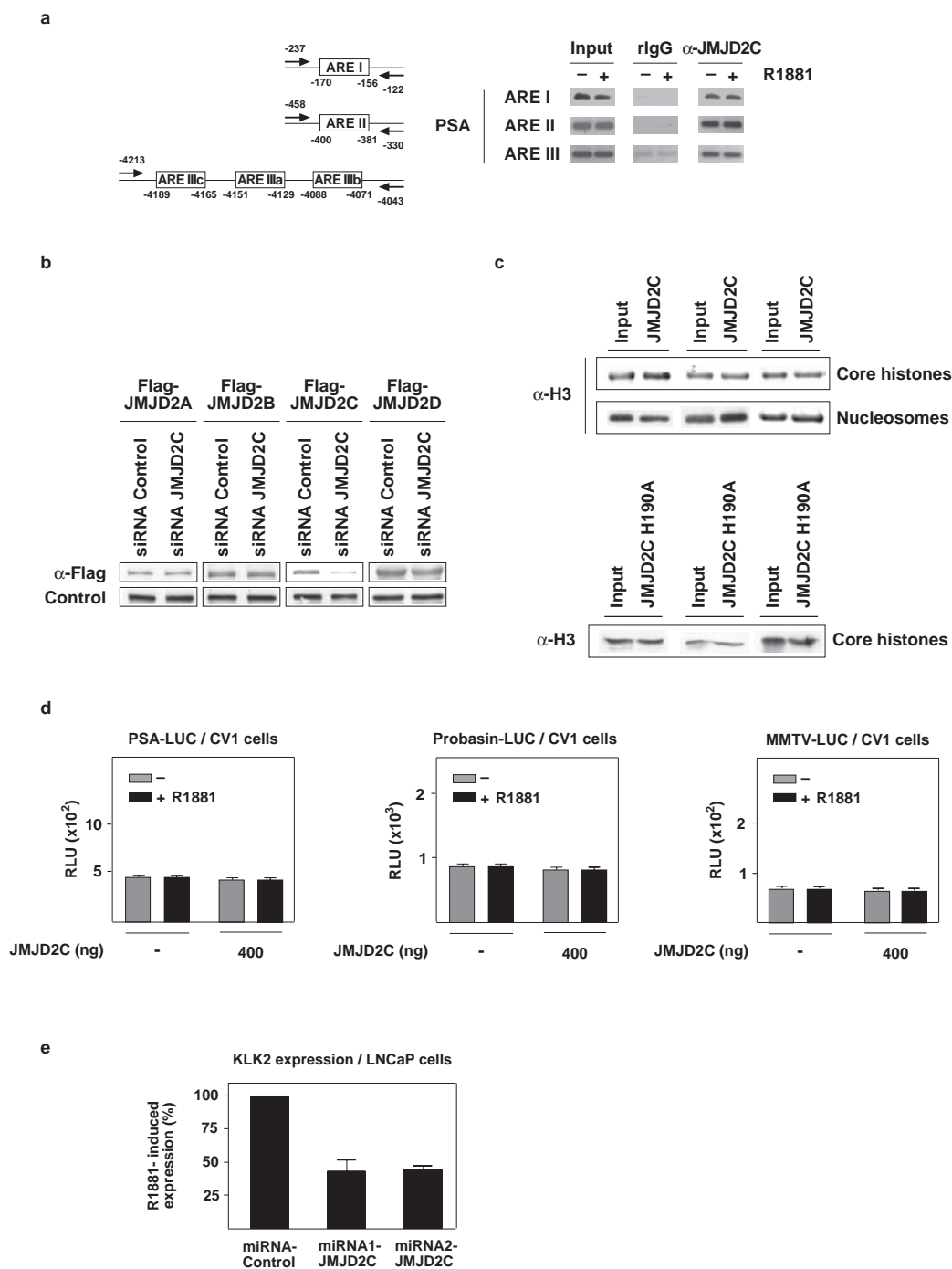
In the letter by Binné *et al.* (*Nature Cell Biol.* **9**, 225–232; 2007), labelling of the molecular weight markers in Fig. 4b was incorrect. This figure has been corrected online and is shown below.





Supplementary Figure S1 a, JMJD2C expression analysis. Confocal laser scanning microscopy shows the sub-cellular localisation of endogenous JMJD2C and AR in human LNCaP prostate tumour cells. AR (red) co-localises with JMJD2C (green) in the nucleus upon addition of the AR agonist R1881. **b**, JMJD2C interacts with AR (left panel) and LSD1 (right panel) *in vivo*. 293 cells were transfected with expression plasmids for V5-JMJD2C and either Flag-AR or Flag (left panel), or V5-JMJD2C and either Flag-LSD1 or Flag (right panel) in the presence of 10^{-10} M R1881 as indicated. Extracts were immunoprecipitated with a-Flag (M2, Sigma) antibody. Five percent of the extract used for immunoprecipitation was loaded as input. Western blots were decorated with a-V5 (Invitrogen; 1:5000) or a-Flag antibody (1:2500). **c**, Association of bacterially expressed AR and JMJD2C *in vitro*. Western blot analysis using α -JMJD2C antibody show that bacterially expressed and purified MBP-JMJD2C interacts with bacterially expressed and purified GST-AR fusion proteins but not with the GST and GST-Nix1 control proteins. (NTD; N-terminal domain, DBD;

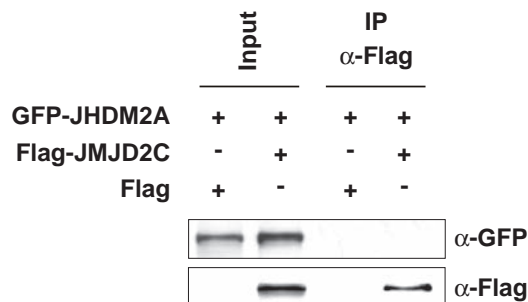
DNA-binding domain, LBD; ligand-binding domain, MBP; maltose-binding protein). 1 percent of the extract used for pull-down was loaded as input. Coomassie blue staining of the amounts of GST fusion proteins used are shown in Figure 1d. **d**, Full-length AR interacts with JMJD2C *in vitro*. MBP pull-down assays were performed with labelled full-length AR (ARwt) and the bacterially expressed and purified MBP-JMJD2C fusion protein. MBP protein was used as control. 1 percent of the extract used for pull-down was loaded as input. Coomassie blue staining shows the amounts of MBP fusion proteins used. **e**, Association of bacterially expressed LSD1 and JMJD2C *in vitro*. Western blot analysis using α -JMJD2C antibody show that bacterially expressed and purified MBP-JMJD2C interacts with bacterially expressed and purified GST-LSD1 and fusion proteins thereof, but not with the GST and GST-Nix1 control proteins. (NTD; N-terminal domain, AO; amine oxidase). 5 percent of the extract used for pull-down was loaded as input. Coomassie blue staining of the amounts of GST fusion proteins used are shown in Figure 1e.



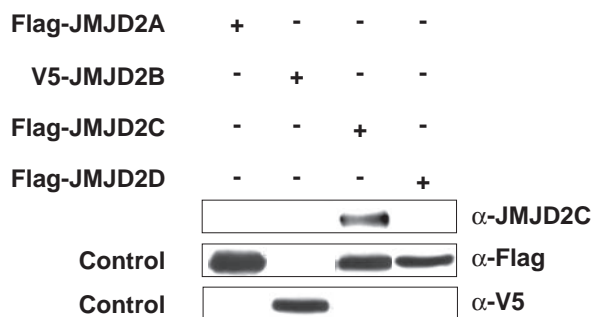
Supplementary Figure S2 a, JMJD2C interacts with chromatin at ARE I, ARE II, and ARE III of the PSA gene. LNCaP cells were incubated with or without the AR agonist R1881. ChIP experiments were performed with α -JMJD2C antibody. The precipitated chromatin was amplified by PCR using primers flanking the promoter region (ARE I (-237/-122) and ARE II (-458/-330)) and the enhancer region (ARE III (-4213/-4043)). Primer sequences are as follows: ARE I (-237/-122): 5'-TTTGTCCCTAGATGAAGTCTCC-3' and 5'-CCCACACCCAGAGCTGTGGAAGG-3', ARE II (-458/-330): 5'-GCCAAGACATCTATTCAGGAGC-3' and 5'-CCTTTGCACTCCA AGACCCAGT-3', ARE III (-4213/-4043): 5'-TGCTCAGCCTTTGTCTCTGATGA-3' and 5'-ATATCTCTCTCAGATCCAGGCTT-3'. **b**, The siRNA mediated knockdown of JMJD2C is specific. 293 cells were transfected with siRNA against JMJD2C

or control siRNA and expression plasmids for human Flag-JMJD2A, Flag-JMJD2B, Flag-JMJD2C, or Flag-JMJD2D. Western blot was decorated with α -Flag antibody (1:2500). **c**, The integrity of core histones and nucleosomes is maintained during the demethylation assay. Core histones or nucleosomes from HeLa cells were incubated with recombinant JMJD2C (aa 12-349) or mutant JMJD2C H190A (aa 12-349). Western blots were decorated with α -H3 antibody. **d**, In the absence of AR, JMJD2C does not induce activation of the AR-regulated reporters PSA-LUC, Probasin-LUC, and MMTV-LUC. CV1 cells were transfected as indicated in the presence or absence of 10^{-10} M R1881. Bars represent mean \pm SD ($n \geq 5$). **e**, miRNA-mediated JMJD2C knockdown reduces ligand-dependent expression of the endogenous *KLK2* gene in LNCaP cells. Bars represent mean \pm SD ($n \geq 4$).

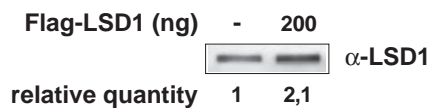
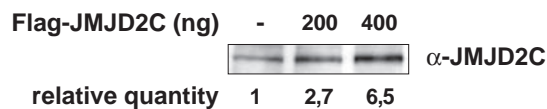
a



b



c



Supplementary Figure S4 a, JMJD2C does not interact with JHDM2A. 293 cells were transfected with expression plasmids for GFP-JHDM2A and either Flag-JMJD2C or Flag. Extracts were immunoprecipitated with α -Flag antibody. Twenty percent of the extract used for immunoprecipitation was loaded as input. Western blots were decorated with α -GFP (Santa Cruz; 1:500) or α -Flag antibody (1:2500). **b**, The α -JMJD2C antibody specifically recognizes JMJD2C. 293 cells were transfected with expression plasmids

for Flag-JMJD2A, V5-JMJD2B, Flag-JMJD2C or Flag-JMJD2D. Western blots were decorated with α -JMJD2C, α -Flag (1:2500) or α -V5 antibody (1:5000). **c**, Expression levels of JMJD2C and LSD1 in CV1 cells. CV1 cells were either mock-transfected or transfected with 200ng or 400ng expression plasmids for Flag-JMJD2C or Flag-LSD1, respectively. Western blots were decorated with α -JMJD2C or α -LSD1 antibody.

Figure 1b

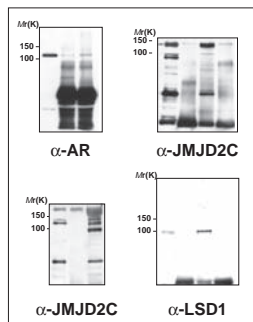


Figure 1c

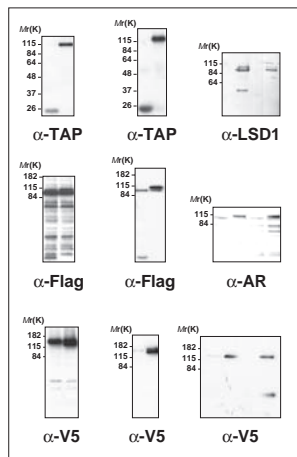


Figure 1d

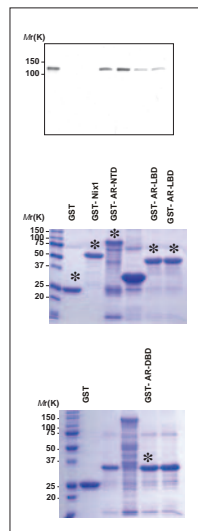


Figure 1e

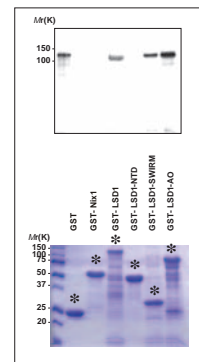


Figure 2c

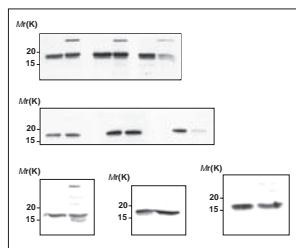


Figure 2b

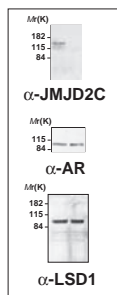
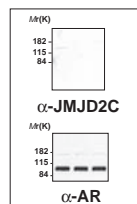


Figure 4a



Supplementary Figure S5 Full scans of gel/western data for Figure 1b, Figure 1c, Figure 1d, Figure 1e, Figure 2c, Figure 2b and Figure 4a.

Immunofluorescence

Cells were analysed essentially as described¹⁶. Primary antibody staining was performed with the indicated dilutions: α-AR 441 (1:5000) and α-JMJD2C (1:250). Sub-cellular localisation was visualised using secondary Alexa Fluor 488- and 546-labelled antibodies (1:4000; Molecular Probes). Nuclei were stained with 1µg/ml DAPI (Roche).

MBP pull-down assay

For maltose-binding protein (MBP)²⁴ pull-down *E.coli* expressed and purified MBP fusion proteins were bound to amylose resin (New England BioLabs). Amylose-bound proteins were incubated with labelled full-length AR following the same protocol as for GST pull-down assays with a buffer containing 100 mM KCl.

24. Busso, D., Delagoutte-Busso, B. & Moras, D. Construction of a set Gateway-based destination vectors for high-throughput cloning and expression screening in *Escherichia coli*. *Anal. Bioch.* **343**, 313-321. (2005).